MTAP Deficiency–Induced Metabolic Reprogramming Creates a Vulnerability to Cotargeting *De Novo* Purine Synthesis and Glycolysis in Pancreatic Cancer

Qiangsheng Hu[1,2,3,4], Yi Qin[1,2,3,4,5], Shunrong Ji[1,2,3,4], Xiuhui Shi[6], Weixing Dai[5], Guixiong Fan[1,2,3,4], Shuo Li[3], Wenyan Xu[1,2,3,4], Wensheng Liu[1,2,3,4], Mengqi Liu[1,2,3,4], Zheng Zhang[1,2,3,4], Zeng Ye[1,2,3,4], Zhijun Zhou[6], Jingxuan Yang[6], Qifeng Zhuo[1,2,3,4], Xianjun Yu[1,2,3,4], Min Li[6], and Xiaowu Xu[1,2,3,4]

ABSTRACT

Methylthioadenosine phosphorylase (MTAP) is a key enzyme associated with the salvage of methionine and adenine that is deficient in 20% to 30% of pancreatic cancer. Our previous study revealed that MTAP deficiency indicates a poor prognosis for patients with pancreatic ductal adenocarcinoma (PDAC). In this study, bioinformatics analysis of The Cancer Genome Atlas (TCGA) data indicated that PDACs with MTAP deficiency display a signature of elevated glycolysis. Metabolomics studies showed that that MTAP deletion–mediated metabolic reprogramming enhanced glycolysis and *de novo* purine synthesis in pancreatic cancer cells. Western blot analysis revealed that MTAP knockout stabilized hypoxia-inducible factor 1α (HIF1α) protein via post-translational phosphorylation. RIO kinase 1 (RIOK1), a downstream kinase upregulated in MTAP-deficient cells, interacted with and phosphorylated HIF1α to regulate its stability. *In vitro* experiments demonstrated that the glycolysis inhibitor 2-deoxy-D-glucose (2-DG) and the *de novo* purine synthesis inhibitor L-alanosine synergized to kill MTAP-deficient pancreatic cancer cells. Collectively, these results reveal that MTAP deficiency drives pancreatic cancer progression by inducing metabolic reprogramming, providing a novel target and therapeutic strategy for treating MTAP-deficient disease.

Significance: This study demonstrates that MTAP status impacts glucose and purine metabolism, thus identifying multiple novel treatment options against MTAP-deficient pancreatic cancer.

Introduction

Pancreatic ductal adenocarcinoma (PDAC) is the second most common gastrointestinal malignancy in the United States, with a five-year survival rate of approximately 10% (1). Clinically, due to early metastasis and invasion to nearby and distal organs in patients with PDAC, the prognosis is poor (2). In addition, drug resistance to traditional chemotherapy and the poor efficacy of targeted therapy drugs also contribute to an unsatisfactory prognosis (3). The different phenotypic characteristics of pancreatic cancers determine tumor proliferation, invasion, metastasis and metabolic reprogramming, and the underlying cause of the different phenotypes lies in genotypic variations (4, 5). PDAC progression develop through a multistage process with the accumulation of loss-of-function mutations of *P53*, *SMAD4*, and *CDKN2A* (6). The *CDKN2A* gene is located at the chromosome 9p21 locus and is proximal to methylthioadenosine phosphorylase (MTAP) in the genome (7). Approximately 15% of all tumor types contain the short-arm deletion of chromosome 9p21 (8), and 80% to 90% of *CDKN2A* gene deletion tumors have homozygous codeletion of MTAP (9). It is worth noting that MTAP deficiency in PDAC has been investigated by Hustinx and colleagues and found to occur in approximately 30% of all analyzed cases (10). The role of CDKN2A in PDAC has been well studied, but MTAP has been much less explored.

MTAP is a key metabolic enzyme involved in the methionine salvage pathway (11). The natural substrate methylthioadenosine (MTA) is catalyzed by MTAP to produce methionine and adenine (12). In MTAP-deficient cancer cells, the salvage pathway for methionine and adenine is absent and caused by decreased MTA catabolism. These components are involved in cellular energy homeostasis, DNA synthesis, and protein synthesis (13). A series of therapeutic strategies have been developed for the metabolic defects in MTAP-deficient tumors, to inhibit tumor progression. For example, MTAP-deficient cells are more susceptible to *de novo* purine synthesis and methionine deprivation inhibitors than MTAP-positive cells (14). Recent studies demonstrated that the absence of MTAP in cancer cells creates vulnerability by targeting the MAT2A/PRMT5/RIO kinase 1 (RIOK1) axis, indicating that this axis may be utilized to develop novel strategies against MTAP-deficient cancers (15–17). These results suggested that MTAP deletion may create metabolic vulnerability with decreased MTA catabolism, which is bad for malignant proliferative cancer cells. However, mounting evidence in cancers such as malignant melanoma, osteosarcoma, gastrointestinal stromal tumors, the Ewing sarcoma family of tumors and lung cancer demonstrates that MTAP deletions confer malignant properties to cancer cells and are associated with an

[1]Department of Pancreatic Surgery, Fudan University Shanghai Cancer Center, Shanghai, China. [2]Department of Oncology, Shanghai Medical College, Fudan University, Shanghai, China. [3]Shanghai Pancreatic Cancer Institute, Shanghai, China. [4]Pancreatic Cancer Institute, Fudan University, Shanghai, China. [5]Cancer Research Institute, Fudan University Shanghai Cancer Center, Shanghai, China. [6]Department of Medicine, Department of Surgery, The University of Oklahoma Health Sciences Center, Oklahoma City, Oklahoma.

Note: Supplementary data for this article are available at Cancer Research Online (http://cancerres.aacrjournals.org/).

Q. Hu, Y. Qin, S. Ji, and X. Shi contributed equally to this article.

Corresponding Authors: Xiaowu Xu, Fudan University Shanghai Cancer Center, Fudan University, Shanghai Pancreatic Cancer Institute, 270 DongAn Road, Shanghai 200032, P.R. China. Phone: 8621-6417-5590; Fax: 8621-6403-1446; E-mail: xuxiaowu@fudanpci.org; and Min Li, Department of Medicine, Department of Surgery, The University of Oklahoma Health Sciences Center, 975 NE 10th Street, BRC 1262A, Oklahoma City, OK 73104. Phone: 405-271-1796; Fax: 405-271-1476; E-mail: Min-Li@ouhsc.edu

Cancer Res 2021;81:4964–80

doi: 10.1158/0008-5472.CAN-20-0414

unfavorable prognosis (18–22). Therefore, it is of high necessity to explore the mechanism by which MTAP deficiency results in defects in MTA metabolism but tends to be associated with more malignant properties. By using pancreatic cancer characterized by high frequencies of MTAP deficiency, we explored the roles of MTAP-loss in governing the metabolism and maintenance of malignancies.

In this study, our survival analysis of The Cancer Genome Atlas (TCGA) dataset revealed that PDAC patients with deep deletion of MTAP displayed worse overall survival (OS) and disease-free survival (DFS) compared with patients without alteration or with amplification of MTAP. Consistent with the TCGA analysis, we demonstrated by IHC staining that patient with lower MTAP expression exhibited worse prognoses. Gene-set enrichment analysis (GSEA) results demonstrated that the glycolysis pathway was the most significantly enriched pathway in patients with PDAC with deep deletion of MTAP. A series of experiments were conducted *in vitro* and *in vivo* further validated the roles of MTAP in glycolytic regulation in pancreatic cancer cells. Our mechanistic study revealed that RIOK1 expression was increased in MTAP-deficient pancreatic cancer cells and that RIOK1 phosphorylates and stabilizes hypoxia-inducible factor 1α (HIF1α). Moreover, metabolomics studies revealed that MTAP-deficient pancreatic cancer cells exhibit increased glycolysis and *de novo* purine synthesis to compensate for the metabolic defects caused by the weakened purine salvage pathway. Finally, we found that the glycolysis inhibitor 2-DG and the *de novo* purine synthesis inhibitor L-alanosine synergized to kill pancreatic cancer cells with MTAP loss. Collectively, these results reveal novel roles of MTAP loss in pancreatic cancer and provide possible targetable molecular mechanisms and strategies for treating MTAP-deficient pancreatic cancer.

Materials and Methods

Cell culture

Human pancreatic cancer cell lines including CFPAC-1, PANC-1, MIA PaCa-2, AsPC-1, and SW1990 cells were purchased from the ATCC in 2018 and were cultured according to standard protocols provided by the ATCC. PANC-1, MIA PaCa-2, and SW1990 cells were cultured in DMEM. AsPC-1 cells were cultured in RPMI1640 medium. CFPAC-1 cells were cultured in IMDM. All cell culture media were supplemented with 10% FBS and 1% antibiotics. Human pancreatic ductal epithelial cell line (HPDE) cells were cultured in keratinocyte serum-free (KSF) medium supplemented with EGF and bovine pituitary extract (Life Technologies; refs. 23, 24). We performed short tandem repeat (STR) profiling to identify all cell lines in this study. All cells were cultured in an incubator with 5% CO_2 at 37°C and confirmed to be free of *Mycoplasma* contamination.

Western blotting

Cells were lysed with RIPA lysis buffer (P0013B, Beyotime Biotechnology Company) supplemented with protease and phosphatase inhibitors (MedChemExpress) for 15 minutes on ice. Protein concentrations in cell lysates were measured with a BCA protein assay kit (P0012, Beyotime Biotechnology Company, Shanghai). Total protein lysates of different samples were separated on 8%–12% SDS-polyacrylamide gels and then electrophoretically transferred to polyvinylidene difluoride (PVDF) membranes (set the power supply to 100V for 1 hour at 4°C). PVDF membranes were blocked with buffer and subsequently incubated with specific antibodies at 4°C overnight or 2 hours at room temperature. The following antibodies were used in this study: anti-β-actin (1:4,000, ab8227, Abcam), anti-MTAP (1:1,000, 11475–1-AP, ProteinTech), anti-HIF1α (1:1,000, 20960–1-AP, ProteinTech), anti-hydroxy-HIF1α (1:1,000, #3434, Cell Signaling Technology), anti-RIOK1 (1:1,000, 17222–1-AP, ProteinTech), anti-Flag (1:5,000, 20543–1-AP, ProteinTech), anti-HA (1:5,000, 51064–2-AP, ProteinTech), anti-phospho-serine (1:1,000, ICP-9806, Nanning Languang Biotechnology) and anti-phospho-threonine (1:1,000, ICP-9807, Nanning Languang Biotechnology).

RNA extraction and quantitative real-time PCR

Total RNA was extracted from cells by using TRIzol reagent (Invitrogen) and subsequently reverse transcribed into cDNA with TaKaRa's Prime Script RT kit. An ABI 7900HT Real-Time PCR system was used to determine the expression status of designated genes by reverse transcription-polymerase chain reaction (RT-PCR). The $2^{-\Delta\Delta C_t}$ method was applied to calculate mRNA expression levels, and the levels were normalized to β-actin. Primers used were listed in Supplementary Table S1.

Plasmids

To overexpress MTAP, $MTAP^{D220A}$, RIOK1, and $RIOK1^{Mut}$ (catalytically dead mutant cDNAs), the pCDH-CMV-MCS-EF1-Puro vector (System Biosciences) was used. The lentiCRISPRv2 vector (Addgene plasmid # 52961) was used to knockout MTAP expression (11, 25). To knockdown RIOK1 and HIF1α, the pLKO.1 TRC cloning vector (Addgene plasmid # 10878) was used (26). The two target sequences for RIOK1 knockdown are GCAGATATGTATCGCATCAAA and CCAGACTGTTACAGGATTGAA, respectively. The target sequence for HIF1α knockdown is CGGCGAAGTAAAGAATCTGAA. Related shRNA- or cDNA-expressing cell pools were selected with puromycin after viral transduction. Related shRNA- or cDNA-expressing cell pools were selected with puromycin after viral transduction.

Cellular assay

To observe the proliferation of cells, we assessed cell viability by using CCK-8 assay, colony formation assay and IC_{50} assessment. Cell viability was assessed with a CCK-8 Kit according to standard protocols provided by the manufacturer (Dojindo Molecular Technologies). At each experimental time point, add 10 μL of CCK-8 solution to each well and incubate for 1–2 hours. Plates were read at 450 nm on a multimode microplate reader. For the colony formation assay, 1,000 cells were plated in 6-well plate and cultured for 14 days. The number of colonies was counted under an inverted microscope. For the IC_{50} assessment, cells were seeded in 96-well plate and treated with the indicated inhibitors (L-alanosine, MCE, HY-16933; 2-deoxy-D-glucose, MCE, HY-13966). The viable cells were counted with the CCK-8 kit, and the absorbance at 450 nm was read on a spectrophotometer. % cytotoxicity = [1 − (absorbance of the experimental well − absorbance of the blank)/(absorbance of the untreated control well − absorbance of the blank)] × 100. We used the above formula for mathematical calculations. The concentration of the drug required to inhibit cell growth by 50% (IC_{50}) was determined by the concentration-response curve.

Tumorigenesis study

BALB/c-nu mice (4–5 weeks of age, 18–20 g, Shanghai Laboratory Animal Center) were housed in sterile, filter-capped cages. 4×10^6 control and MTAP-overexpressing MIA PaCa-2 cells in 100 μL of PBS were injected subcutaneously into the left and right flanks of mice. The flanks of six other mice were injected subcutaneously with 4×10^6 CFPAC-1 cells (right/MTAP-knockout and left/MTAP wild type) in 100 μL PBS. Five weeks after implantation of the subcutaneous tumor,

the mice were prepared for microPET/CT scanning after 6–8 hours of fasting. After scanning, we euthanized the mice and removed the subcutaneous tumors intact. The animal experiments in this study were performed strictly in accordance with the guidelines for the care and use of experimental animals and were approved by IACUC of Fudan University (Shanghai, China).

MicroPET/CT imaging

An Inveon MicroPET/CT instrument (Siemens Medical Solutions) was used for MicroPET/CT scanning and image analysis. Each mouse with subcutaneous tumor was injected with 11.1 MBq (300 μCi) of 18F-FDG via the tail vein. The mice were anesthetized with isoflurane for microPET/CT scanning starting at 2 hours after injection. Inveon Research Workplace was used to obtain the percentage injected dose per gram (%ID/g) and SUVs. The SUV_{max} was calculated using standard methods according to our previous report (27). We included six subcutaneous tumors in each experimental group and the control group for statistical analysis of SUV_{max} value.

Metabolism assays

To investigate whether MTAP deletion regulates glycolysis and mitochondrial respiration in pancreatic cancer cells, we performed the extracellular acidification rate (ECAR) measurements and the oxygen consumption rate (OCR) measurements using Seahorse Extracellular Flux analyzer according to the manufacturer's instructions for the Seahorse Glycolysis Stress Test Kit and XF Cell Mito stress test kit.

Gas chromatography time-of-flight mass spectrometry (GC-TOF/MS) and liquid chromatography-coupled tandem mass spectrometry (LC-MS/MS) were performed to measure small-molecule metabolites followed by unsupervised hierarchical clustering. Metabolomics assays were conducted by Metabo-Profile (28). Data were analyzed using the iMAP platform (v1.0; Metabo-Profile) and MetaboAnalyst 4.0 (29). The whole relationship was visualized using a Z-score heat map.

Tumor glucose uptake analysis of patients with pancreatic cancer

SUV_{max} reflected glucose uptake capacity by assessing 18F-FDG uptake via PET/CT imaging. To investigate the correlation between MTAP expression level and glucose uptake, we collected the SUV_{max} data of tumors in patients with pancreatic cancer. The SUV_{max} was calculated according to our previous reports (27).

Measurement of HIF1α protein half-life

To assess the protein stability of HIF1α, cycloheximide was used to inhibit protein synthesis, and protein lysates were harvested at the indicated time points. Western blotting for HIF1α and β-actin were performed, and the band intensities were quantified using ImageJ software (30).

Protein interaction assay

The protein interactions were validated via a co-immunoprecipitation (co-IP) assay (31), and protein colocalization in the cells was confirmed via Immunofluorescence (32). For the co-IP assays, cells were washed with ice-cold PBS and solubilized in RIPA lysis buffer (P0013B, Beyotime Biotechnology Company) that contained protease and phosphatase inhibitors. An equal amount of each protein lysate was incubated with the indicated antibody (anti-HIF1α polyclonal antibody, 20960–1-AP, ProteinTech; anti-RIOK1 polyclonal antibody, ab88496, Abcam; anti-Flag, 20543–1-AP Proteintech; anti-HA, 51064–2-AP, Proteintech) for 6–8 hours at 4°C, followed by incubation with Pierce Protein A/G magnetic beads for another 2 hours. After washing 4–6 times to eliminate nonspecific protein binding, the immune complexes were performed Western blot analysis after denaturation in SDS-loading buffer. For the immunofluorescence experiments, cells were plated onto glass coverslips. We used 4% paraformaldehyde to fixed pancreatic cancer cells. The cells were permeabilized with 0.1% Triton X-100 and blocked for 1 hour at room temperature in PBS containing 1% BSA. The cells were then incubated with the indicated primary antibodies (anti-HIF1α antibody, 1:100, ab179483, Abcam; RIOK1 polyclonal antibody, 1:500, ab254723, Abcam) in blocking buffer at 4°C for overnight. After washing three times with PBS, the cells were then incubated with the indicated fluorophore-conjugated secondary antibodies at room temperature for another 1 hour. After washing with PBS, the cells were mounted with antifade solution with DAPI. The localization status of the indicated proteins was observed using Confocal Microscopy. For GST pull-down experiments, we generated recombinant His-tagged RIOK1 and GST-tagged HIF1α proteins in bacteria. The expression plasmids pET28a-RIOK1 and pGEX-4T-1-HIF1α were transformed into BL21 (DE3) cells and induced with IPTG to produce the relevant proteins. GST pulldown assays were performed as described previously (33).

Synergy

Synergism between 2-DG and L-alanosine were assessed using the Chou-Talalay method with CompuSyn software (34).

Tissue specimens and IHC staining

Clinical information of TMAs samples was acquired from patients with PDAC who underwent surgical resection at Fudan University Shanghai Cancer Center (FUSCC). All of the patients were informed written consent and the studies were conducted in accordance with the Declaration of Helsinki ethical guidelines and approved by the Institutional Research Ethics Committee of FUSCC. Postoperative follow-ups were conducted by Huanyu Xia. MTAP and HIF1α expression levels were calculated by multiplying the positivity and intensity scores according to our previous report (35). The expression levels according to the results of IHC scoring were classified as follows: negative (0, −), weakly positive (1–4, +), moderately positive (6–8, ++), and strongly positive (9–12, +++). Then, the patients were divided into two groups (scores < 6, low expression; scores ≥ 6, high expression). IHC staining of MTAP and HIF1α were performed according to standard procedures. Slides were deparaffinized, rehydrated, and treated with 3% H_2O_2. Antigen retrieval was performed in a pressure cooker for 15 minutes in Antigen Retrieval Citra Solution. The slides were then incubated with peroxidase blocking reagent for 15 minutes. After blocking for 1 hour at room temperature, the slides were incubated with the indicated antibodies for 8–12 hours or overnight at 4°C. After washing with PBS, the slides were incubated with the secondary antibody at 37°C for 30 minutes. Next, streptavidin biotin complex HRP-conjugated reagents were added to the samples and incubated at 37°C for 30 minutes. The slides were washed with PBS. After incubated with DAB reagent, the tissue staining intensity was monitored under a bright-field microscope, and the slides were then washed with distilled water. The staining intensities were evaluated by three blinded pathologists. Antibodies used for IHC staining were purchased from Abcam (anti-MTAP antibody, ab126770, 1:200) and ProteinTech (HIF1α polyclonal antibody, 20960–1-AP, 1:200).

TCGA and bioinformatics analysis

The DNA copy number and RNA-sequencing expression data from TCGA dataset (http://www.cbioportal.org/) were analyzed. Patients

without copy number or mRNA expression data were excluded. Differentially expressed genes (DEGs) between patients with or without MTAP copy number alterations were compared by DESeq analysis. Gene Set Enrichment Analysis (GSEA) was further performed to reveal the biological pathways involved in pancreatic cancer progression in patients stratified by the MTAP copy number status. The Kaplan-Meier curve comparing the survival of patients with or without MTAP copy number alterations was estimated using the log-rank test.

Statistical analysis

GraphPad Prism 7.0 software and SPSS software (version 22.0; IBM Corporation) were used for all statistical analyses. Statistical analyses were performed using a two-tailed Student *t* test to evaluate the significance of the differences between two groups. For multiple comparisons, the Tukey-Kramer honestly significant difference test was applied following one-way analysis of variance (ANOVA). Pearson correlation analysis was used to determine the correlation between the expression of two indicated molecules. Data are reported as the mean ± SD from three independent experiments. Kaplan-Meier analysis and log-rank tests were used to analyze OS and DFS. Differences were considered significant at *, $P < 0.05$; **, $P < 0.01$; ***, $P < 0.001$.

Results

Deep MTAP gene deletion is prevalent in patients with PDAC and associated with a poor prognosis

The gene encoding MTAP lies on chromosome 9p21 and is flanked by CDKN2A, which encodes p16 and p14ARF (**Fig. 1A**). MTAP is homozygously deleted in 27% to 42% of pancreatic cancers and other solid tumors, as evidenced via analysis of the TCGA dataset at http://www.cbioportal.org/ (**Fig. 1B**; refs. 36, 37). In addition, the mRNA level of MTAP was analyzed based on a TCGA dataset. Forty-three of 177 patients (24.3%) showed deep deletions, 62 of 177 patients (35.0%) showed LOH, and 72 of 177 patients (40.7%) showed nonalteration (69/72) or amplifications (3/72). Combined analysis of the mRNA and copy-number variation (CNV) data confirmed that deep deletion of MTAP was correlated with strikingly reduced mRNA levels (**Fig. 1C**). Further survival analysis revealed that patients with deep deletion of MTAP had significantly poorer long-term OS (**Fig. 1D**) and DFS (**Fig. 1E**) than patients without alteration or with amplification of MTAP. Subsequently, we assessed MTAP expression for the prediction of OS and DFS in pancreatic cancer. According to the IHC staining score, the patients were divided into High MTAP group and Low MTAP group (**Fig. 1F**). By using IHC staining of MTAP, we demonstrated that 26.5% of the patients from the FUSCC cohort displayed an absence of MTAP expression, similar to the deletion frequency observed in the TCGA cohort (**Fig. 1G**). In addition, the OS and DFS analyses of the FUSCC cohort revealed that the patients with lower MTAP expression levels had worse prognoses (**Fig. 1H** and **I**).

The metabolic pathway of glycolysis is significantly enriched in PDAC patients with deep deletion of MTAP

To gain further insights into the biological processes and signaling pathways associated with CNVs of MTAP, GSEA was performed in TCGA datasets. The gene expression profiles of patients with deep deletion, loss of heterozygosity (LOH) and nonalteration/amplification of MTAP are listed in **Fig. 2A**. GSEA enrichment plots showed that the metabolic pathway of glycolysis was the most significantly enriched pathway in patients with deep deletion of MTAP (**Fig. 2B** and **C**). Glycolysis is a multistep process catalyzed by different glycolytic enzymes (38, 39). Key enzymes in glycolysis were selected and compared between patients with different expression statuses of MTAP. The patients with deep deletion of MTAP exhibited increased expression levels of glycolytic enzymes (**Fig. 2D**). Collectively, these results indicated that patients with MTAP deficiency may exhibit a stronger glycolytic phenotype than those with intact MTAP.

MTAP negatively regulates glycolysis by decreasing HIF1α stability in pancreatic cancer

To confirm the GSEA results indicating the roles of MTAP in glycolytic regulation, we manipulated MTAP expression in pancreatic cancer cells and examined its impact on glycolysis *in vitro* and *in vivo*. First, we examined the status of MTAP expression in pancreatic cancer cell lines and human pancreatic ductal epithelial cell lines, including CFPAC-1, MIA PaCa-2, PANC-1, AsPC-1, SW1990 and HPDE (**Fig. 3A**). We selected two cell lines for subsequent studies: CFPAC-1, with MTAP expression, and MIA PaCa-2, which contains a homozygous MTAP deletion. MTAP was silenced via the CRISPR tool in CFPAC-1 cells and was overexpressed in MIA PaCa-2 cells via lentivirus-mediated transfection (**Fig. 3B**). CFPAC-1 cells were also exposed to methylthio-DADMe-immucillin A (MTDIA, 10 μmol/L, HY-101496 from MCE), which inhibit MTAP enzymatic activity. Aspartate 220 is a critical residue necessary for enzyme activity at the MTAP catalytic site (40). We created a novel MIA PaCa-2 cell line that stably expressed $MTAP^{D220A}$ and thus was unable to exert the enzyme activity of MTAP (**Fig. 3B**). By using Agilent extracellular flux analyzer to measure glucose metabolism, we demonstrated that CFPAC-1 cells with MTAP deficiency or MTDIA treatment had higher levels of glycolysis, while forced expression of MTAP rather than $MTAP^{D220A}$ in MIA PaCa-2 cells suppressed glycolysis (**Fig. 3C** and D; Supplementary Fig. S1A). Our results suggested that MTAP deletion or MTDIA treatment induced an obvious decrease in the OCR value in CFPAC-1 cells. In addition, in MIA PaCa-2 cells, overexpression of MTAP increased the OCR value, while overexpression of $MTAP^{D220A}$ had little effect on the OCR value (**Fig. 3E** and **F**; Supplementary Fig. S1B). These results indicate that the enzymatic activity of MTAP is closely related to its regulation of glycolysis in pancreatic cancer cells. Subsequently, we used MTAP-deficient CFPAC-1 cells and MTAP-overexpressing MIA PaCa-2 cells to establish subcutaneous xenograft mouse models and analyzed 18F-FDG uptake with PET/CT. The 18F-FDG uptake results demonstrated that silencing MTAP increased 18F-FDG uptake and that overexpressing MTAP decreased 18F-FDG uptakel, further reinforcing the negative roles of MTAP in glycolysis (**Fig. 3G** and **H**). Finally, we studied the relationship between MTAP expression in tumor tissues from patients with PDAC and the ability of tumor glucose uptake, as reflected on PET/CT scans. Patients with lower levels of MTAP displayed higher maximum standardized uptake values (SUV_{max}; **Fig. 3I**). Consistent with the GSEA results, these data demonstrated that MTAP deficiency may confer a glycolytic advantage on pancreatic cancer cells to meet the demand for malignant biological behavior. HIF1α is an important molecule that regulates glycolysis in malignant tumors (41). According to the GSEA results, MTAP deletion results in the enrichment of HIF1α-targeted genes in glycolytic processes. Therefore, we sought to determine whether MTAP could regulate HIF1α expression. We observed that neither MTAP knockout nor MTDIA treatment affected HIF1α mRNA levels in CFPAC-1 cells, and similarly, overexpression of MTAP or $MTAP^{D220A}$ in MIA PaCa-2 cells did not change HIF1α mRNA levels (**Fig. 3J**; Supplementary Fig. S1C). However, whether after knocking out MTAP or after MTDIA treatment, we observed a significant upregulation of HIF1α

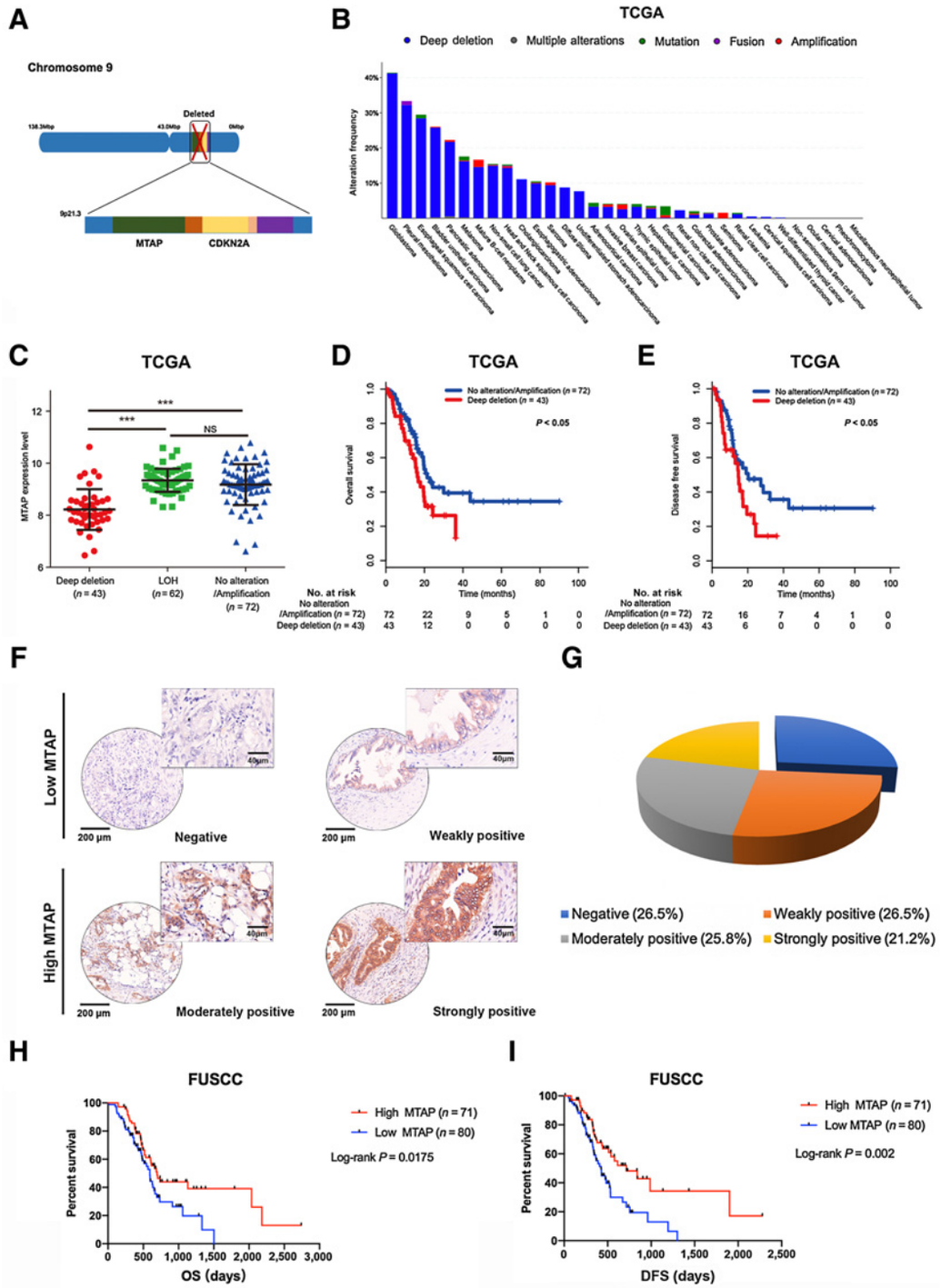

Figure 1.

Deep MTAP gene deletion is prevalent in patients with PDAC and is associated with a poor prognosis. **A,** Schematic depicting the chr9 and chr9p21.3 regions containing the MTAP gene close to the CDKN2A gene. **B,** MTAP was deleted in pancreatic cancer and other solid tumors in a dataset from TCGA. **C,** The transcriptional levels of different MTAP mutation states, including the deep deletion group, loss of heterozygosity (LOH) group, and no alteration/amplification group, were analyzed based on the TCGA dataset. **D** and **E,** Long-term overall survival and disease-free survival were significantly worse in patients with deep deletion of MTAP than in patients without alteration or with amplification of MTAP in the TCGA datasets. Kaplan–Meier analysis and log-rank tests were used to analyze OS and DFS. **F,** The expression of MTAP was assessed in pancreatic cancer patients. **G,** In total, 26.5% of the patients in the FUSCC cohort exhibited an absence of MTAP expression, similar to the deletion frequency in the TCGA cohort. **H** and **I,** Overall survival (OS) and disease-free survival (DFS) analyses of the FUSCC cohort demonstrated that patients with lower MTAP expression displayed worse prognoses.

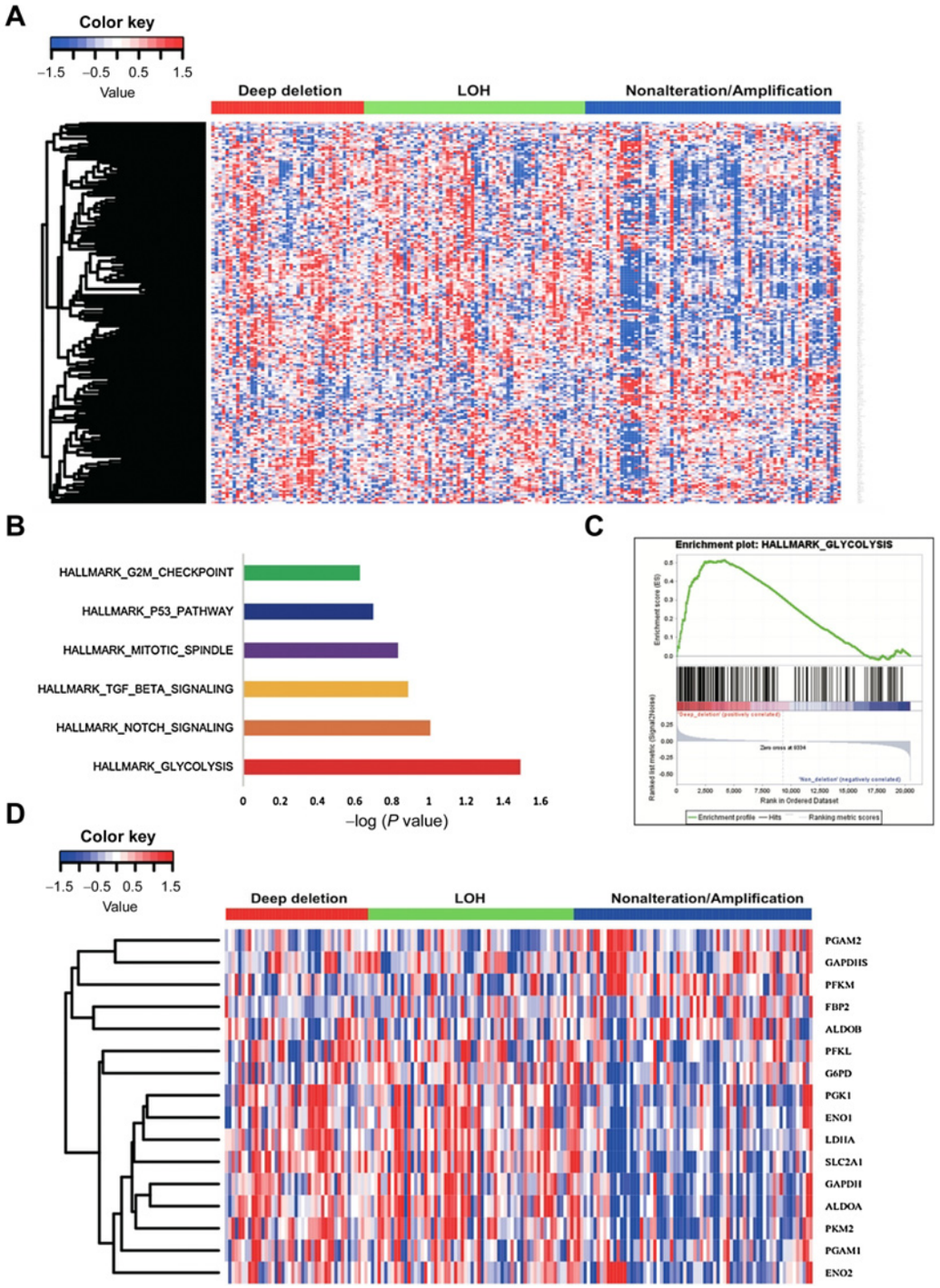

Figure 2.

The metabolic pathway of glycolysis is significantly enriched in PDAC patients with deep deletion of MTAP. **A,** The gene expression profiles of patients with deep deletion, LOH, and nonalteration/amplification of MTAP are listed. **B** and **C,** GSEA enrichment plots show that the metabolic pathway of glycolysis was the most significantly enriched pathway in patients with deep deletion of MTAP. **D,** Key enzymes in glycolysis were selected and compared between patients with different expression statuses of MTAP.

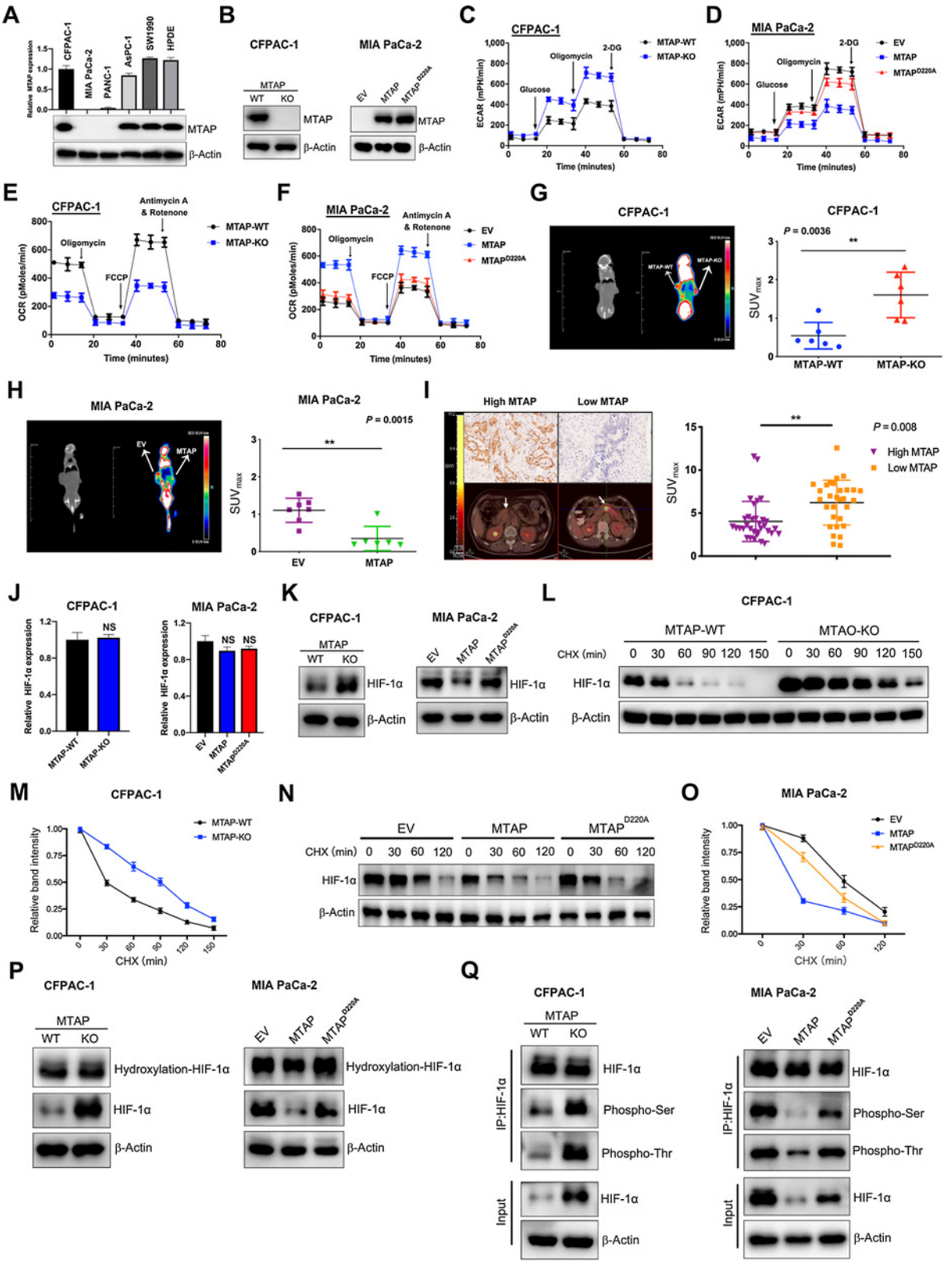

protein levels in CFPAC-1 cells (**Fig. 3K**, left; Supplementary Fig. S1D). Furthermore, introduction of wild-type MTAP into MIA PaCa-2 cells inhibited HIF1α protein levels, while overexpression of the enzyme-dead form of MTAP did not inhibit HIF1α protein levels (**Fig. 3K**, right). Subsequently, we performed a half-life assay of HIF1α in pancreatic cancer cells by inhibiting protein synthesis with cycloheximide. In CFPAC-1 cells, silencing MTAP expression or treatment with MTDIA increased HIF1α protein stability (**Fig. 3L** and **M**; Supplementary Fig. S1E and S1F), while in MIA PaCa-2 cells, overexpressing MTAP but not $MTAP^{D220A}$ significantly decreased HIF1α stability (**Fig. 3N** and **O**). This pattern prompted us to evaluate whether MTAP could regulate HIF1α posttranslationally. Posttranslational hydroxylation and phosphorylation account for HIF1α protein stability. Therefore, we examined the impact of MTAP on the hydroxylation and phosphorylation of HIF1α. Whether we knocked out MTAP or inhibited its enzymatic activity with MTDIA in CFPAC-1 cells or overexpressed MTAP in MIA PaCa-2 cells, we observed slight changes in HIF1α hydroxylation (**Fig. 3P**; Supplementary Fig. S1G). Similarly, overexpression of $MTAP^{D220A}$ in MIA PaCa-2 cells did not significantly affect the hydroxylation of HIF1α. However, we demonstrated that silencing MTAP or treating with MTDIA increased serine and threonine residues phosphorylation of HIF1α. However, overexpression of MTAP, but not $MTAP^{D220A}$, decreased the phosphorylation of HIF1α (**Fig. 3Q**; Supplementary Fig. S1H). Furthermore, we observed that silencing HIF1α expression reversed the metabolic reprogramming caused by MTAP-KO in CFPAC-1 cells (Supplementary Fig. S1I–S1K). Finally, we demonstrated by IHC staining that MTAP is negatively correlated with HIF1α expression in patients with PDAC (Supplementary Fig. S2A and S2B). Collectively, these results demonstrated that MTAP can posttranslationally regulate HIF1α protein stability and then regulate HIF1α-mediated glycolysis.

RIOK1, a kinase downstream of MTAP deletion, interacts with HIF1α and regulates its stability to regulate glucose metabolism in pancreatic cancer

HIF1α can be regulated by post-translational phosphorylation. The kinase RIOK1 is strongly required for the growth of MTAP-deficient cancer cells based on a previous report (15). Therefore, we sought to determine whether MTAP could regulate HIF1α protein stability via RIOK1. First, we observed that knockout of MTAP or treatment with MTDIA in CFPAC-1 cells caused RIOK1 to be upregulated at the transcriptional and translational levels (**Fig. 4A** and **B**, left and Supplementary Fig. S2C and S2D). Consistent with this result, overexpression of MTAP but not $MTAP^{D220A}$ in MIA PaCa-2 cells reduced the expression level of RIOK1 (**Fig. 4A** and **B**/right). RIOK1 is a novel component of the PRMT5 complex that interacts directly with PRMT5 in cancer cells. It has been shown that PRMT5 is inhibited by the accumulation of the metabolite MTA in tumors with MTAP loss (42). Interestingly, the interaction between RIOK1 and PRMT5 was decreased while the interaction between RIOK1 and HIF1α was increased in MTAP-loss CFPAC-1 cells compared with WT cells (Supplementary Fig. S3A). We investigated the mRNA and protein levels of RIOK1 in various PDAC cell lines and HPDE cells (Supplementary Fig. S3B). We also detected the protein level of HIF1α in these cells. We observed that RIOK1 and HIF1α expression levels were downregulated in MTAP-WT PDAC cells and HPDE cells compared with MTAP-deficient PDAC cells. Therefore, we speculated that the increased phosphorylation of HIF1α in MTAP-deficient pancreatic cancer cells was regulated by RIOK1. We further observed colocalization of RIOK1 and HIF1α in MIA PaCa-2 cells and human pancreatic ductal adenocarcinoma tissue sections (**Fig. 4C** and **D**). To validate the interaction between RIOK1 and HIF1α, CFPAC-1 cells were transfected with $RIOK1^{HA}$. RIOK1 and HIF1α were found to interact with each other in Co-IP experiments (**Fig. 4E**). This interaction was further confirmed between endogenous RIOK1 and HIF1α in MIA PaCa-2 cells (**Fig. 4F**). Our *in vitro* pull-down assay further indicated that RIOK1 directly bound to HIF1α (**Fig. 4G**). To investigate whether the direct binding of RIOK1 to HIF1α can affect the phosphorylation of HIF1α, we cotransfected $RIOK1^{HA}$ with $HIF1\alpha^{FLAG}$ in HEK293T cells and observed that the Ser/Thr phosphorylation of HIF1α was increased (**Fig. 4H**). To clarify the regulatory effect of RIOK1 on the phosphorylation level of HIF1α, we created RIOK1 shRNA MIA PaCa-2 cells, as well as RIOK1wt rescue and RIOK1 active site (D324N) and ATP binding domain (K208R) catalytically inactive mutant (15, 43, 44) CFPAC-1 cells. RIOK1 silencing and overexpression efficiencies were evaluated by qPCR and Western blot analysis (Supplementary Fig. S3C-S3D). Not $RIOK1^{Mut}$ (catalytically dead mutant cDNAs) but RIOK1-WT introduction increased the phosphorylation of HIF1α (**Fig. 4I**). However, silencing RIOK1 in MIA PaCa-2 cells decreased Ser/Thr phosphorylation of HIF1α (**Fig. 4J**). By using cycloheximide to inhibit protein synthesis and monitor protein stability, we demonstrated that introduction of RIOK1-WT but not $RIOK1^{Mut}$ increased the protein stability of HIF1α (**Fig. 4K** and **L**).

Figure 3.

MTAP negatively regulates glycolysis in pancreatic cancer cells. **A,** Western blot and quantitative real-time PCR analyses of the indicated human pancreatic cancer cell lines and HPDE cells. **B,** MTAP was knocked out in CFPAC-1 cells via the CRISPR tool and overexpressed in MIA PaCa-2 cells via lentivirus-mediated transfection. **C–F,** The knockout of MTAP expression in CFPAC-1 cells and the overexpression of wild-type MTAP but not $MTAP^{D220A}$ in MIA PaCa-2–induced metabolic reprogramming, as reflected by the ECAR and OCR. **G** and **H,** Representative ^{18}F-FDG microPET/CT images of tumor-bearing mice. The xenografts with CFPAC-1 (MTAP-WT and MTAP-KO) cells and MIA PaCa-2 (EV and MTAP) cells are indicated with white arrows. The ratios of the xenograft SUV_{max} in the MTAP-KO group ($n = 6$) and the MTAP-WT group ($n = 6$). The ratios of the xenograft SUV_{max} in the MTAP group ($n = 6$) and the parent group ($n = 6$). **I,** Representative ^{18}F-FDG PET/CT images of PDAC patients with high or low MTAP expression. Patients with lower levels of MTAP displayed higher SUV_{max} values. Analysis of the SUV_{max} of patients with PDAC in the high MTAP ($n = 33$) and low MTAP ($n = 30$) groups. **J,** Quantitative real-time PCR analysis of HIF1α mRNA levels in CFPAC-1 (MTAP-WT and MTAP-KO) and MIA PaCa-2 (EV and MTAP and $MTAP^{D220A}$) cells. **K,** Western blot analysis of HIF1α protein levels in CFPAC-1 (MTAP-WT and MTAP-KO) and MIA PaCa-2 (EV and MTAP and $MTAP^{D220A}$) cells. **L,** CFPAC-1 (MTAP-WT and MTAP-KO) cells were treated with 20 μg/mL cycloheximide (CHX), and whole-cell lysates were collected at the indicated time points for immunoblot analysis. **M,** Line chart of relative band intensity for the indicated times. Semiquantification with β-actin as a loading control and relative HIF1α protein levels at time 0 were set as 1. **N,** MTAP- or $MTAP^{D220A}$-overexpressing MIA PaCa-2 cells and the corresponding control cells were treated with cycloheximide (20 μg/mL) for the indicated durations, and the protein levels of HIF1α were determined by Western blotting. **O,** Line chart of relative band intensity for the indicated times. Overexpression of MTAP, but not $MTAP^{D220A}$, decreased the protein stability of HIF1α in MIA PaCa-2 cells. **P,** Immunoblot analysis of hydroxylated HIF1α and HIF1α in CFPAC-1 (MTAP-WT and MTAP-KO) and MIA PaCa-2 (EV and MTAP and $MTAP^{D220A}$) cells. MTAP silencing in CFPAC-1 cells and overexpression in MIA PaCa-2 cells did not significantly influence the hydroxylation of HIF1α. **Q,** Immunoprecipitation (IP) analysis revealed increased phosphorylated HIF1α on serine and threonine residues and increased HIF1α protein levels in MTAP-KO CFPAC-1 cells compared with WT control cells. Overexpression of MTAP but not $MTAP^{D220A}$ significantly decreased phosphorylated HIF1α on serine and threonine residues in MIA PaCa-2 cells. Data are shown as the mean ± SD from three independent experiments performed in triplicate. NS, nonsignificant; **, $P < 0.01$.

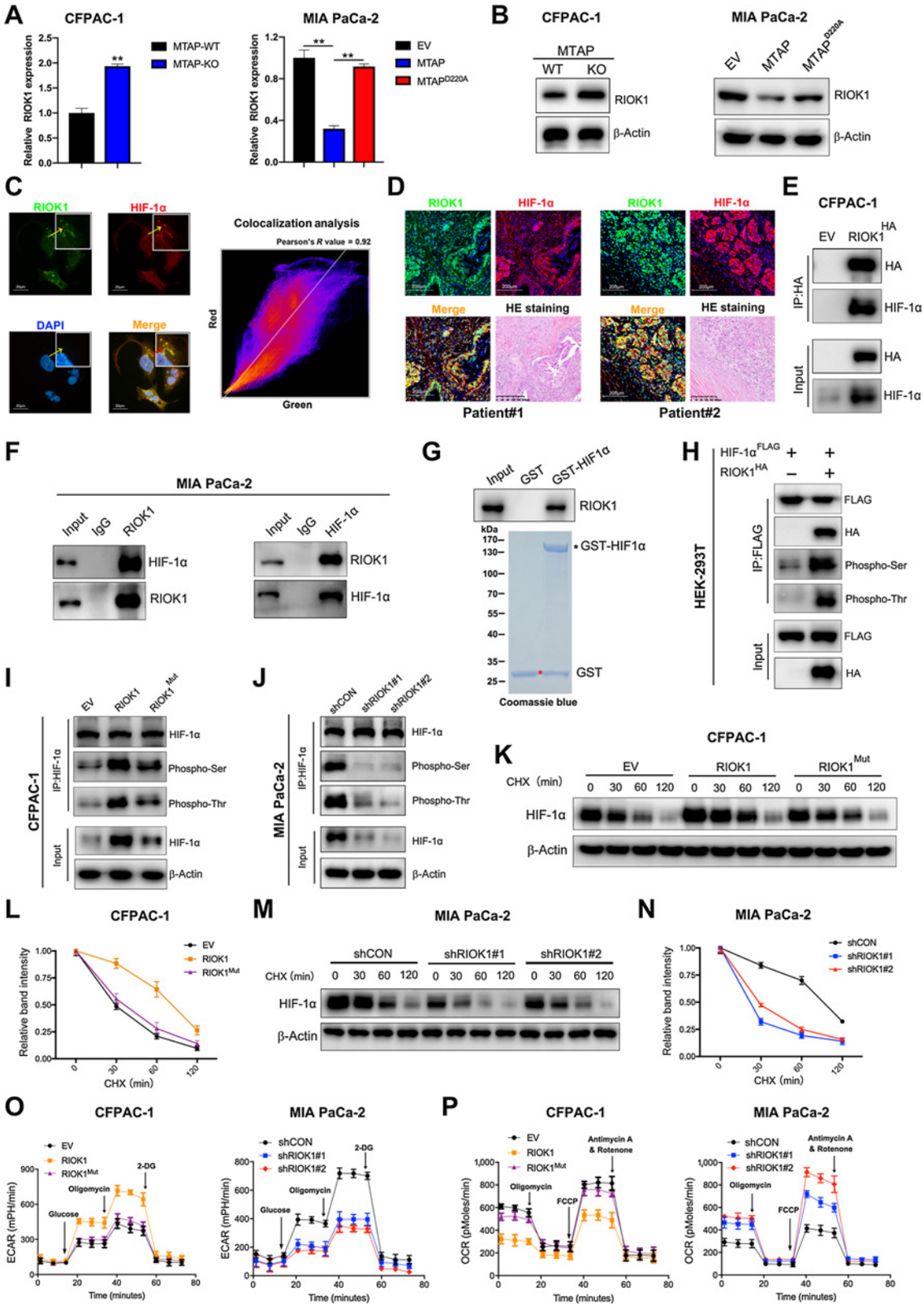

However, silencing RIOK1 decreased the protein stability of HIF1α in MIA PaCa-2 cells (**Fig. 4M** and **N**). Finally, we discovered an obvious increase in the ECAR value and a decrease in the OCR value in CFPAC-1 cells with the introduction of RIOK1-WT but not RIOK1^{Mut} (**Fig. 4O** and **P**, left). At the same time, we also observed that silencing RIOK1 inhibited glycolysis but promoted mitochondrial respiration in MIA PaCa-2 cells by using Agilent extracellular flux analyzer (**Fig. 4O** and **P**, right). Using a CCK-8 kit, we have observed that RIOK1 can promote the proliferation of pancreatic cancer cells (Supplementary Fig. S3E and S3F).

MTAP is involved in the regulation of HIF1α and glucose metabolism via RIOK1 in pancreatic cancer cells

To further clarify that MTAP regulates the phosphorylation of HIF1α through RIOK1, we performed immunoblot assays and demonstrated that overexpressed or silenced RIOK1 can rescue the change in the HIF1α levels caused by MTAP overexpression or silencing in MIA PaCa-2 and CFPAC-1 cells, respectively (**Fig. 5A** and **B**). By using cycloheximide to inhibit protein synthesis and monitor protein stability, we demonstrated that in MTAP wild-type CFPAC-1 cells, silencing MTAP increased the protein stability of HIF1α, while simultaneous silencing of RIOK1 attenuated the increase in HIF1α stability caused by MTAP knockout (**Fig. 5C** and **D**). However, simultaneous introduction of RIOK1 mitigated the decrease in HIF1α stability caused by MTAP overexpression in MIA PaCa-2 cells (**Fig. 5E** and **F**). Next, we further investigated whether the upregulation of glycolysis induced by MTAP deletion was mediated by RIOK1. In CFPAC-1 cells, silencing MTAP increased glycolysis levels and glycolytic capacity, while simultaneous silencing of RIOK1 attenuated the increase in glycolysis caused by MTAP knockout (**Fig. 5G**). Cotransfection of MTAP with RIOK1 in MIA PaCa-2 cells had a consistent reverse effect on the ECAR value based on results obtained from Agilent extracellular flux analyzer (**Fig. 5H**). Similarly, intervention with RIOK1 expression also reversed the regulatory effect of MTAP on mitochondrial respiration in CFPAC-1 and MIA PaCa-2 cells (**Fig. 5I** and **J**).

Metabolomics analysis confirmed that glycolytic and *de novo* purine synthesis metabolites are significantly increased in MTAP-deficient pancreatic cancer cells

To explore the direct impact of MTAP deficiency on metabolic reprogramming, we performed metabolomics analysis to measure the levels of metabolites regulated by MTAP knockout in both CFPAC-1 cells and CFPAC-1 subcutaneous tumor cells (**Fig. 6A**). Via metabolic pathway enrichment analysis (MPEA), we demonstrated that the glycolysis pathway is among the significantly altered pathways in MTAP-KO cells compared with controls (**Fig. 6B**). The significantly altered metabolic pathways also included the pentose phosphate pathway and the purine metabolism pathway. Because MTAP is a key enzyme involved in the cysteine and methionine metabolism pathway, it is not surprising that this pathway was significantly altered. Glycolysis-related genes were evaluated by RT-PCR and were found to have increased levels of transcription after MTAP knockout in CFPAC-1 cells (Supplementary Fig. S4A). We also found that silencing HIF1α recovered the increase of genes involved in glycolysis caused by MTAP deficiency. Accordingly, overexpression of MTAP in MIA PaCa-2 cells decreased the expression of these genes (Supplementary Fig. S4B). Further LC/MS-MS metabolomics analysis demonstrated that MTAP deficiency caused an increase in the levels of metabolites in glycolysis and the pentose phosphate pathway (**Fig. 6C** and **D**). MTAP salvages purines by releasing adenine from MTA, a byproduct of the polyamine biosynthetic pathway. In MTAP-deficient cells, defects in the salvage synthesis pathway enhanced *de novo* purine synthesis. Consistent with these findings, we observed an increase in metabolites in the *de novo* purine synthesis pathway (**Fig. 6E**). Collectively, these results prompted us to propose that MTAP deficiency can induce metabolic reprogramming by enhancing the Warburg effect and pentose phosphate pathway to accelerate *de novo* purine biosynthesis (**Fig. 6F**).

2-DG synergizes with L-alanosine to kill pancreatic cells with MTAP deficiency

MTAP-null pancreatic cancer cells lack the ability to salvage purine synthesis and are therefore more vulnerable to inhibition of *de novo* purine synthesis; this finding was verified by Landon J. Hansen and colleagues in glioblastoma (11). In previous studies, we found that the increased *de novo* purine synthesis is closely related to the abnormally elevated level of glycolysis, therefore, we aimed to determine whether glycolysis could be a therapeutic target in MTAP-deficient pancreatic cancer cells. First, we observed that MTAP knockout significantly upregulated the protein levels of GLUT1 and HK2 in CFPAC-1 cells (**Fig. 7A**), which is consistent with the changes in their transcription levels. In addition, glucose uptake by MTAP-deficient CFPAC-1 cells was significantly increased to meet the demand for robust glycolysis metabolism (**Fig. 7B**). 2-Deoxy-D-glucose (2-DG) is a glucose analogue that can act as a competitive inhibitor of glucose metabolism (45).

Figure 4.

RIOK1, a kinase downstream of MTAP deletion, interacts with HIF1α and regulates its stability to regulate glucose metabolism in pancreatic cancer. **A,** qPCR analysis of RIOK1 expression in CFPAC-1 (MTAP-WT and MTAP-KO) cells and MIA PaCa-2 cells infected with an empty vector or MTAP- and MTAP^{D220A}-expressing virus. β-Actin mRNA expression was used as an internal control. **B,** Knockout of MTAP in CFPAC-1 cells increased the protein level of RIOK1. Overexpression of MTAP in MIA PaCa-2 cells significantly inhibited RIOK1 protein levels, but overexpression of the MTAP mutant with no enzymatic activity did not significantly inhibit RIOK expression. **C,** Colocalization of RIOK1 and HIF1α in MIA PaCa-2 cells by immunofluorescence microscopy. Scale bar, 20 μm. A statistical analysis of the fluorescence images is added to the right of the fluorescence image. **D,** Colocalization of RIOK1 and HIF1α in primary tumor sections from patients with human pancreatic cancer observed by immunofluorescence. Scale bar, 200 μm. **E,** We found that RIOK1 can interact with HIF1α by utilizing a co-IP assay in CFPAC-1 cells. **F,** The endogenous binding proteins of RIOK1 and HIF1α in MIA PaCa-2 cells. **G,** Western blot analysis of RIOK1 binding to purified GST and GST-tagged HIF1α using RIOK1 antibody (top). GST and GST-tagged HIF1α were visualized by staining with Coomassie brilliant blue R-250 (bottom). The red and black asterisks are GST- and GST-tagged HIF1α, respectively. **H,** In HEK293T cells, cotransfection of HIF1α^{FLAG} with RIOK1^{HA} increased Ser/Thr residue phosphorylation of HIF1α. **I,** Immunoprecipitation (IP) analysis of the indicated proteins revealed that RIOK1-WT but not RIOK1^{Mut} (RIOK1 K208R/D324N catalytically dead mutant cDNA) introduction significantly increased the phosphorylation of HIF1α in CFPAC-1 cells. **J,** Silencing RIOK1 in MIA PaCa-2 cells decreased Ser/Thr residue phosphorylation of HIF1α. **K** and **L,** Cells were treated with 20 μg/mL cycloheximide (CHX), and whole-cell lysates were collected at the indicated time points for immunoblot analysis. Introduction of RIOK1-WT but not RIOK1^{Mut} increased the protein stability of HIF1α. **M,** MIA PaCa-2 cells with RIOK1 knockdown and the corresponding control cells were treated with cycloheximide (20 μg/mL) for the indicated durations, and the protein levels of HIF1α were determined by Western blotting. **N,** Silencing RIOK1 in MIA PaCa-2 cells decreased the protein stability of HIF1α. **O** and **P,** Introduction of RIOK1-WT but not RIOK1^{Mut} increased the ECAR value and decreased the OCR value in CFPAC-1 cells. Silencing RIOK1 reduced the ECAR value and upregulated the OCR value in MIA PaCa-2 cells. Data are shown as the mean ± SD from three independent experiments performed in triplicate. **, $P < 0.01$.

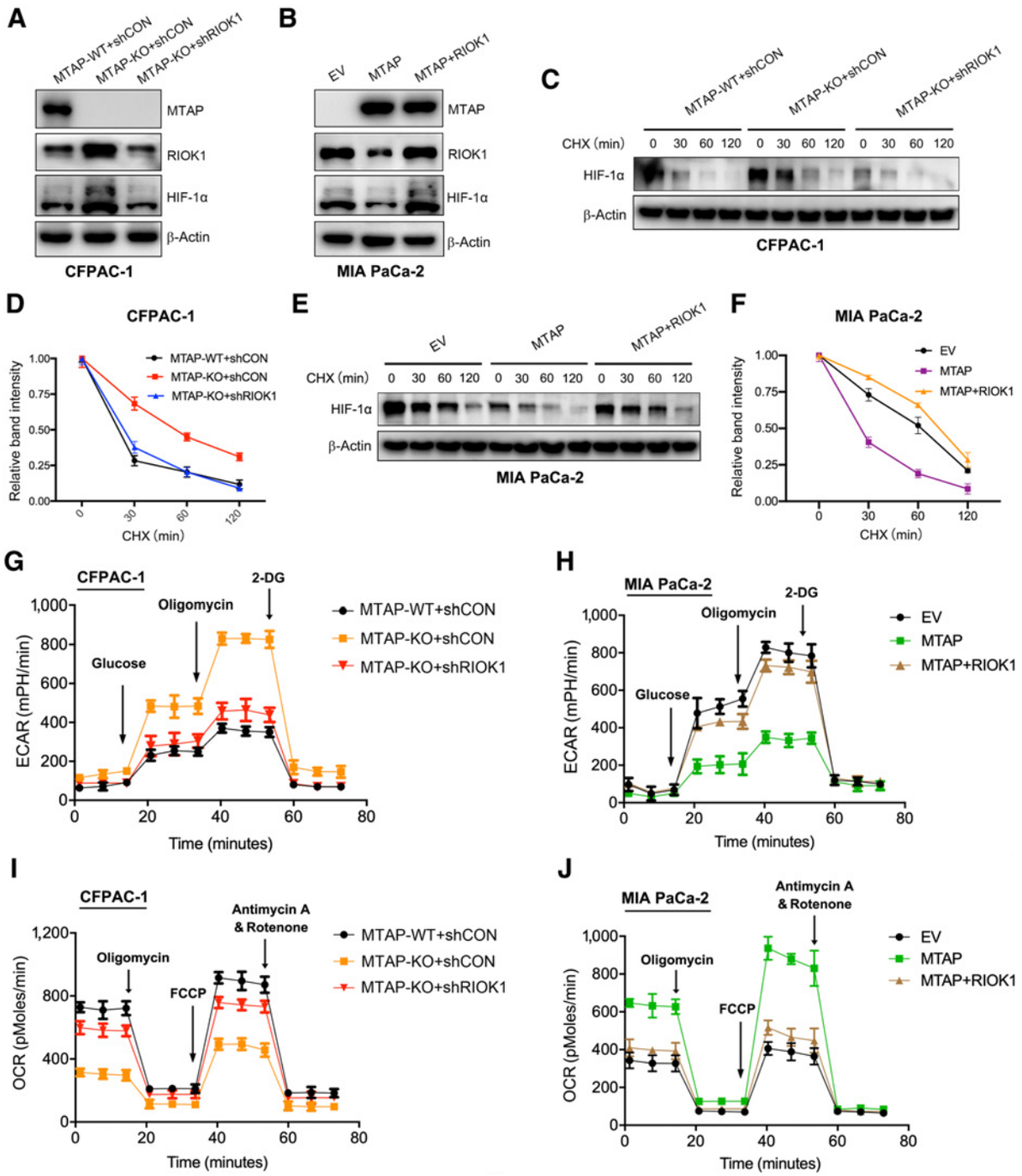

Figure 5.

MTAP is involved in the regulation of HIF1α and glucose metabolism via RIOK1 in pancreatic cancer cells. **A,** Western blot analysis indicated that knockdown of RIOK1 expression could reverse the upregulation of HIF1α protein levels induced by MTAP deficiency in CFPAC-1 cells. **B,** RIOK1 rescued the change in HIF1α levels caused by MTAP overexpression in MIA PaCa-2 cells. **C** and **D,** In MTAP wild-type CFPAC-1 cells, MTAP silencing increased the protein stability of HIF1α, while simultaneous RIOK1 silencing attenuated the increase in HIF1α stability caused by MTAP knockout. **E** and **F,** Overexpression of MTAP in MIA PaCa-2 cells decreased the stability of HIF1α, and simultaneous introduction of RIOK1 mitigated the decrease in HIF1α stability caused by MTAP. **G,** A Seahorse extracellular flux analyzer was used to measure the ECAR, and the results indicated that simultaneous silencing of RIOK1 attenuated the increase in glycolysis level and glycolytic capacity caused by MTAP knockout. **H,** A Seahorse extracellular flux analyzer was used to measure the ECAR, and the results indicated that overexpression of MTAP in MIA PaCa-2 cells decreased glycolysis levels, and simultaneous introduction of RIOK1 mitigated the decrease in glycolysis levels caused by MTAP. **I,** Silencing of RIOK1 reversed the decrease in the OCR value induced by MTAP knockout in CFPAC-1 cells. **J,** Introduction of RIOK1 attenuated the increase in the OCR value caused by MTAP in MIA PaCa-2 cells. Data are shown as the mean ± SD from three independent experiments performed in triplicate.

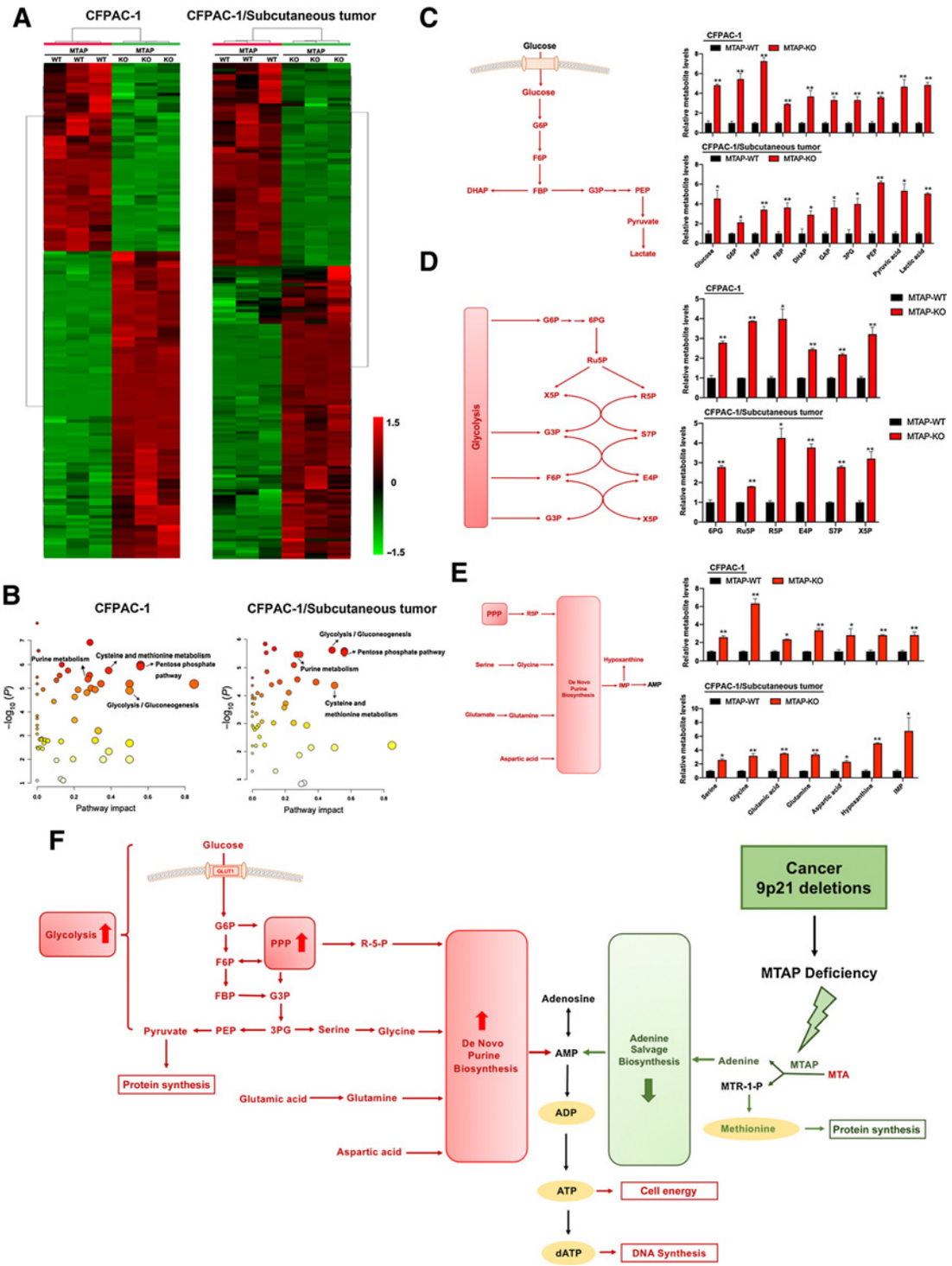

Figure 6.

Metabolomics analysis confirmed that glycolytic and *de novo* purine synthesis metabolites are significantly increased in MTAP-deficient pancreatic cancer cells. **A,** Unsupervised hierarchical clustering of significantly deregulated metabolites between CFPAC-1 cells and CFPAC-1 subcutaneous tumor cells. **B,** Metabolic pathway impact analysis of significantly upregulated metabolites by MetaboAnalyst 4.0. **C,** Major metabolites altered in the glycolytic pathway. **D,** Pentose phosphate pathway metabolite levels in CFPAC-1 cells and CFPAC-1 subcutaneous tumor cells based on LC-MS/MS metabolomics. **E,** Levels of metabolites of the *de novo* purine synthesis pathway determined by LC-MS/MS-based metabolomics. **F,** Schematic representation revealed that the loss of MTAP enhances the glycolytic pathway and promotes the pentose phosphate pathway (PPP) to promote metabolic flux in *de novo* purine synthesis. *, $P < 0.05$; **, $P < 0.01$; ***, $P < 0.001$.

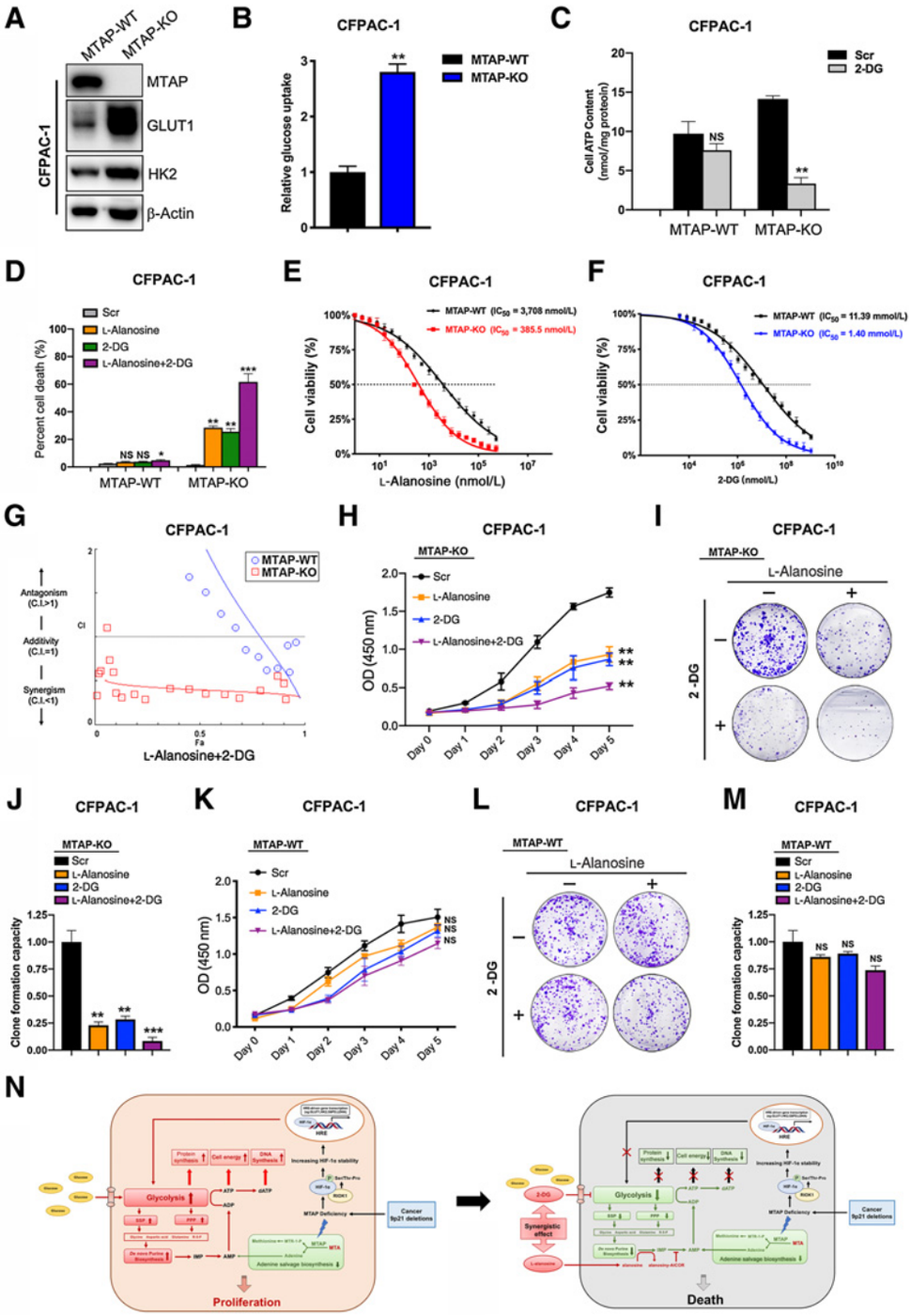

Figure 7.

2-DG synergizes with L-alanosine to kill CFPAC-1 pancreatic cells with MTAP deficiency. **A,** Western blot analysis indicated a significant increase in the protein levels of GLUT1 and HK2 after MTAP knockout in CFPAC-1 cells. **B,** MTAP knockout CFPAC-1 cells had increased glucose utilization, as assessed by glucose uptake. **C,** 2-DG treatment significantly reduced the level of ATP in MTAP-knockout CFPAC-1 cells but not MTAP wild-type CFPAC-1 cells. **D,** Treatment with the combination of L-alanosine (200 nmol/L) and 2-DG (1 mmol/L) significantly promoted the death of MTAP-deficient CFPAC-1 cells but not MTAP wild-type CFPAC-1 cells. **E** and **F,** Knockout of MTAP significantly increased the sensitivity of CFPAC-1 cells to L-alanosine (385 nmol/L vs. 3708 nmol/L) and 2-DG (1.4 mmol/L vs. 11.39 mmol/L) compared with WT controls. **G,** Combined utilization of 2-DG and L-alanine exerted synergistic lethal effects in MTAP-deficient CFPAC-1 cells. **H–M,** Both CCK-8 and colony formation assays showed that treatment with either L-alanosine or 2-DG significantly inhibited the proliferation of MTAP-deficient CFPAC-1 cells, and the combination of the two inhibitors had the most obvious inhibitory effect. **N,** Schematic representation of the working model. Data are shown as the mean ± SD from three independent experiments performed in triplicate. NS, nonsignificant; **, $P < 0.01$.

The high expression of GLUT1 and HK2 in MTAP-deficient pancreatic cancer cells provides sufficient preconditions for 2-DG to inhibit glycolytic metabolism. 2-DG is imported into cancer cells by GLUT1 and then phosphorylated by HK2 to be converted into 2-DG-6-phosphate, a toxic byproduct that inhibits glycolysis (46). We observed that 2-DG treatment significantly reduced the level of ATP in MTAP-KO CFPAC-1 cells compared with MTAP-WT CFPAC-1 cells (**Fig. 7C**). In addition, compared with treatment with each inhibitor alone, treatment with the combination of 2-DG and L-alanosine significantly promoted the death of MTAP-knockout CFPAC-1 cells but not MTAP wild-type CFPAC-1 cells (**Fig. 7D**). By determining the IC_{50} value, we found that the loss of MTAP significantly increased the sensitivity of CFPAC-1 cells to L-alanosine and 2-DG (**Fig. 7E** and **F**). Furthermore, to assess the interaction between L-alanosine and 2-DG, the combination index (CI) values were calculated to obtain *in vitro* cytotoxicity data for the combination of L-alanosine and 2-DG in MTAP-loss and MTAP wild-type CFPAC-1 cells. According to Chou theory, CI (47) values less than, equal to, or greater than 1 could indicate that L-alanosine and 2-DG interact synergistically, additively, or antagonistically, respectively. We concluded that the combination of 2-DG and L-alanine exerted synergistic lethal effects on MTAP-KO CFPAC-1 cells (**Fig. 7G**). We further found via CCK-8 and colony formation assays that treatment with either L-alanosine or 2-DG significantly inhibited the proliferation of MTAP-KO CFPAC-1 cells and that treatment with the combination of these two inhibitors had the most obvious inhibitory effect (**Fig. 7H–J**). We also observed that L-alanosine and 2-DG could not significantly inhibit the proliferation of MTAP wild-type CFPAC-1 cells (**Fig. 7K–M**). In MIA PaCa-2 cells, we conducted a similar investigation. Overexpression of MTAP decreased the protein levels of GLUT1 and HK2 as well as glucose uptake (Supplementary Fig. S5A and S5B). We observed that 2-DG treatment could not significantly reduce the level of ATP in MTAP-WT rescue MIA PaCa-2 cells (Supplementary Fig. S5C). We confirmed the synergistic lethal effects of L-alanosine and 2-DG on MIA PaCa-2 cells with MTAP deficiency (Supplementary Fig. S5D-S5G). Interestingly, we observed that knocking down the expression of RIOK1 in MIA PaCa-2 cells significantly increased the sensitivity to L-alanosine but did not significantly increase the sensitivity to 2-DG (Supplementary Fig. S5H and S5I). We speculated that knockdown of RIOK1 could inhibit glycolysis in cancer cells, resulting in reduced uptake of 2-DG and, thus, weakening the tumor-suppressive effect of 2-DG. We also observed that L-alanosine and 2-DG could not effectively inhibit HPDE cells (Supplementary Fig. S6A and S6B), which suggested that the combined regimen can protect normal pancreatic cells from damage while treating MTAP-deficient pancreatic cancer cells. Finally, the colony formation assays were repeated with MTAP-KO and shRIOK1 CFPAC-1 cells and MTAP and RIOK1 MIA PaCa-2 cells (Supplementary Fig. S7A–S7D). Therefore, we conclude that due to the stabilizing effect of RIOK1 on HIF1α, the glycolysis level of MTAP-deficient pancreatic cancer cells was upregulated, providing a prerequisite for the anticancer effect of L-alanosine combined with 2-DG.

Discussion

In summary, we showed that the loss of MTAP, a key enzyme involved in the salvage of both methionine and adenine, enhances the Warburg effect and increases cell vulnerability by cotargeting *de novo* purine synthesis and glycolysis in pancreatic cancer (**Fig. 7N**). Metabolic reprogramming from glycolysis to *de novo* purine synthesis meets the demands of nucleic acids and ATP to sustain the proliferation of MTAP-null pancreatic cancer cells. These observations explain why pancreatic cancer patients with MTAP deficiency display a worse prognosis than patients with wild-type MTAP. Our results regarding MTAP are consistent with the finding verified by Hansen and colleagues in glioblastoma (11); specifically, these authors demonstrated that MTAP deletion promotes glioblastoma pathogenesis by shaping the epigenetic landscape and stemness of glioblastoma multiforme cells. However, the finding by Hansen and colleagues was very recently challenged by Menezes and colleagues (48). Their findings suggested that the loss of MTAP has no predictive significance for the prognosis of gliomas and that MTAP is not a typical tumor suppressor gene in gliomas. We believe that MTAP, as a key metabolic enzyme, has different metabolic remodeling effects in different types of tumors, which may be due to diversified tumor cell metabolism patterns. In pancreatic cancer cells, one of the hallmarks is cellular energetics characterized by the Warburg effect. It has been known for decades that the glycolytic flux of cancer cells increases significantly even in the presence of oxygen and normal mitochondrial function (49). Through this study, we found that MTAP-deficient pancreatic cancer cells can stabilize HIF1α and activate its downstream glycolysis to meet the energy requirements for malignant proliferation. Therefore, we believe that MTAP is involved in regulating the malignant biological behavior of pancreatic cancer.

MTAP expression is reported to be reduced in many tumors. It is hypothesized that L-alanosine kills MTAP-null solid tumors based on its inhibitory effect on *de novo* purine biosynthesis. However, a phase II trial from multicenter studies using L-alanosine for the treatment of MTAP-null cancers, including mesothelioma, pancreatic cancer, non-small cell lung cancer (NSCLC), soft tissue sarcoma and osteosarcoma, displayed limited effects on preselected patients (50). We believe that the use of L-alanosine alone is not sufficient to kill MTAP-null pancreatic cancer cells because increased glucose metabolism can provide raw materials for nucleic acid synthesis, thus weakening the antitumor effect of L-alanosine. Considering our results, we believe that pancreatic cancer cells with MTAP loss are vulnerable to synthetic lethal metabolic strategies in which L-alanosine induces the inhibition of *de novo* purine synthesis, whereas 2-DG suppresses the compensatory reliance of purine synthesis on the Warburg effect. These *in vitro* experiments confirmed that the glycolytic inhibitor 2-DG can inhibit the growth of MTAP-deficient pancreatic cancer cells and synergize with L-alanosine. Similarly, the effects of combining the glycolysis inhibitor 2-DG with toxic nucleotides used to interfere with nucleic acid metabolism remain to be explored. In addition, it is necessary to explore strategies to leverage the relationship between methionine metabolism remodeling and abnormal glycolysis as a therapeutic vulnerability in MTAP-null pancreatic cancer cells. For example, studies assessing whether the glycolytic inhibitor 2-DG and methionine metabolism inhibitors, such as MAT2A inhibitors, have synergistic lethal effects on MTAP-deficient cells are warranted in the future. Because MTAP deletion does not occur in normal pancreatic ductal epithelial cells, the therapeutic agents targeting MTAP deletion used in this study are both targeted and relatively safe. Our *in vitro* experiments also confirmed that L-alanosine and 2-DG had no significant inhibitory effect on normal HPDE cells.

The role of MTAP in glycolysis and *de novo* purine synthesis has been studied by several groups (38, 51, 52). Other recent studies demonstrated that the absence of MTAP in cancer cells creates vulnerability by targeting the RIOK1 axis (15, 16). Although many studies have been conducted because of the biological importance of MTAP, few have explored the crosstalk between these findings. We

confirmed that constitutive activation of the RIOK1/HIF1α axis in MTAP-null pancreatic cancer cells caused abnormal glycolysis. Previous studies have reported that RIOK1 is associated with PRMT5 based on its subsequent methylation of biomolecules (53). We found that the interaction between PRMT5 and RIOK1 could be disrupted, as the methylation activity of PRMT5 is inhibited in MTAP-deficient cells caused by MTA accumulation. Therefore, HIF1α competes with PRMT5 for interaction with RIOK1. Competitive binding to RIOK1 leads to HIF1α phosphorylation and subsequent stabilization. Using catalytically dead point mutants of RIOK1, we demonstrated that the catalytic activity of the enzyme is critical for stabilizing HIF1α levels to upregulate glycolysis and provide energy for the proliferation of MTAP-deficient PDAC cells. We confirmed that MTAP loss caused a compensatory increase in RIOK1 levels in pancreatic cancer cells and explained why RIOK1 is selectively required for the proliferation of MTAP-deficient cancer cells from a new perspective of glycolysis metabolism rather than methionine metabolism. Interestingly, it is the phosphorylation modification that affects the stability of HIF1α rather than the hydroxylation modification mediated by EGLNs in most cases. Intracellular phosphorylation can flexibly respond to the level of cell energy metabolism, and it can also regulate the activation and stability of the HIF1α protein. MAPKs probably phosphorylate the HIF1α protein, which could activate it (54). Soitamo and colleagues found that the redox state of the cells influences the function of HIF1α and its stability, DNA binding, and phosphorylation (55). The importance of oxygen-dependent and ubiquitin-mediated HIF-1 regulatory subunit (HIF1α) proteolysis was first reported in 1997. Since then, increasing evidence has shown that even under normoxic conditions, HIF1α may become stable and active (56). We suggest that phosphorylation of HIF1α in malignant tumors may be critical in maintaining stability under normoxia. El-Deiry and colleagues reported that CDK1 directly interacts with and phosphorylates HIF1α in an oxygen-independent manner (57). The mechanisms by which phosphorylation increases HIF1α protein stability involve both proteasomal and/or lysosomal degradation. Yang Liuqing and colleagues proved that LINK-A and two protein kinases, BRK and LRRK2, cooperate to mediate a growth factor-triggered signaling cascade to synergistically increase the phosphorylation and stabilization of the HIF1α protein under normoxia (58). Although we have confirmed that RIOK1 can phosphorylate HIF1α and promote its stability, it cannot be ruled out that phosphorylation causes an increase in the transcriptional activity of HIF-1a and thus promotes downstream gene expression. Therefore, further studies are required to confirm the impact of RIOK1 on HIF1α transcriptional activity regulation. The role of RIOK1 in cancer promotion in various malignancies (59, 60) may also be related to its regulation of glycolytic metabolism. In addition, the specific mechanism by which MTAP regulates RIOK1 requires further study. The main methyl donor, SAM is a universal substrate for all methylation reactions in cancer cells, including DNA methylation. DNA methylation is widely used as a "silent" epigenetic marker for transcriptional repression. Deletion of MTAP leads to downregulation of intracellular SAM levels (61). We speculated that the decrease in histone and DNA methylation in the RIOK1 promoter region caused by the deletion of MTAP may be one of the reasons for the upregulation of RIOK. Interestingly, RIOK1 depletion was also shown to block the proliferation of EGFR-driven and Ras-mutated cancer cells in various cancers (59, 62). Of note, 95% of pancreatic ductal adenocarcinomas carry an activating KRAS mutation. Therefore, RIOK1 inhibitors have good research prospects for the treatment of pancreatic cancer. We hope that we can utilize this type of biomarker-directed approach, such as combination treatment with pharmacologic inhibitors of RIOK1 and L-alanosine, to selectively block the growth of MTAP-deficient cancers.

MTAP is always homozygously codeleted with the neighboring *CDKN2A* gene, which encodes the tumor suppressor protein p16. p16 is a cyclin-dependent kinase inhibitor that locks retinoblastoma tumor suppressor protein (Rb) in its active, antiproliferative state (63). CDKN2A loss accompanied by MTAP deletion promotes both Rb phosphorylation and subsequent progression into the S-phase of the cell cycle (64). Aberrant cell-cycle progression caused by p16 deletion requires a large amount of deoxyribonucleotides to support DNA synthesis to sustain uncontrolled proliferation. Codeletion of CDKN2A and MTAP may not only be a naturally occurring event due to proximity in the genomic locus (20) but also have physiologic impacts. CDKN2A deletion disrupts fine-tuned cell-cycle progression, leading to uncontrolled proliferation. Moreover, codeletion of MTAP governs metabolic reprogramming from glycolysis to nucleic acid synthesis required for DNA synthesis to meet the demand for proliferation. However, the impact of p16 deletion on the metabolic remodeling of MTAP-deficient cells warrants further study. More investigations and explorations are required to examine the impact of p16 on metabolic reprogramming with the aim of developing novel strategies and targets against pancreatic cancer.

Authors' Disclosures

No disclosures were reported.

Authors' Contributions

Q. Hu: Conceptualization, data curation, software, formal analysis, validation, investigation, visualization, methodology, writing–original draft, writing–review and editing. **Y. Qin:** Conceptualization, data curation, software, funding acquisition, validation, investigation, methodology, writing–original draft. **S. Ji:** Conceptualization, data curation, software, formal analysis, validation, visualization. **X. Shi:** Conceptualization, software, formal analysis, visualization, writing–review and editing. **W. Dai:** Data curation, software, validation, writing–review and editing. **G. Fan:** Software, formal analysis, validation, methodology, writing–review and editing. **S. Li:** Data curation, software, methodology, writing–review and editing. **W. Xu:** Data curation, supervision, writing–review and editing. **W. Liu:** Software, methodology, writing–review and editing. **M. Liu:** Data curation, software, validation, writing–review and editing. **Z. Zhang:** Formal analysis, methodology, writing–review and editing. **Z. Ye:** Data curation, investigation, methodology, writing–review and editing. **Z. Zhou:** Writing–review and editing. **J. Yang:** Writing–review and editing. **Q. Zhuo:** Writing–review and editing. **X. Yu:** Conceptualization, supervision, funding acquisition, project administration, writing–review and editing. **M. Li:** Conceptualization, supervision, writing–review and editing. **X. Xu:** Conceptualization, supervision, funding acquisition, project administration, writing–review and editing.

Acknowledgments

The authors thank Huanyu Xia for providing assistance with the clinical data collection. This research was supported by the Scientific Innovation Project of Shanghai Education Committee (2019-01-07-00-07-E00057) and National Science Foundation for Distinguished Young Scholars of China (81625016 to X. Yu); National Natural Science Foundation of China (81871950 to Y. Qin); and National Natural Science Foundation of China (81972250 to X. Xu).

The costs of publication of this article were defrayed in part by the payment of page charges. This article must therefore be hereby marked *advertisement* in accordance with 18 U.S.C. Section 1734 solely to indicate this fact.

Received March 29, 2020; revised May 18, 2021; accepted August 11, 2021; published first August 12, 2021.

References

1. Siegel RL, Miller KD, Jemal A. Cancer statistics, 2019. CA Cancer J Clin 2019;69:7–34.
2. Moyer MT, Gaffney RR. Pancreatic adenocarcinoma. N Engl J Med 2014;371:2140.
3. Deplanque G, Demartines N. Pancreatic cancer: are more chemotherapy and surgery needed? Lancet 2017;389:985–6.
4. Makohon-Moore A, Iacobuzio-Donahue CA. Pancreatic cancer biology and genetics from an evolutionary perspective. Nat Rev Cancer 2016;16:553–65.
5. Schneider G, Schmid RM. Genetic alterations in pancreatic carcinoma. Mol Cancer 2003;2:15.
6. Hezel AF, Kimmelman AC, Stanger BZ, Bardeesy N, Depinho RA. Genetics and biology of pancreatic ductal adenocarcinoma. Genes Dev 2006;20:1218–49.
7. Hamid A, Petreaca B, Petreaca R. Frequent homozygous deletions of the CDKN2A locus in somatic cancer tissues. Mutat Res 2019;815:30–40.
8. Bertino JR, Waud WR, Parker WB, Lubin M. Targeting tumors that lack methylthioadenosine phosphorylase (MTAP) activity: current strategies. Cancer Biol Ther 2011;11:627–32.
9. Zhang H, Chen ZH, Savarese TM. Codeletion of the genes for p16INK4, methylthioadenosine phosphorylase, interferon-alpha1, interferon-beta1, and other 9p21 markers in human malignant cell lines. Cancer Genet Cytogenet 1996;86:22–8.
10. Hustinx SR, Hruban RH, Leoni LM, Iacobuzio-Donahue C, Cameron JL, Yeo CJ, et al. Homozygous deletion of the MTAP gene in invasive adenocarcinoma of the pancreas and in periampullary cancer: a potential new target for therapy. Cancer Biol Ther 2005;4:83–6.
11. Hansen LJ, Sun R, Yang R, Singh SX, Chen LH, Pirozzi CJ, et al. MTAP loss promotes stemness in glioblastoma and confers unique susceptibility to purine starvation. Cancer Res 2019;79:3383–94.
12. Zappia V, Della Ragione F, Pontoni G, Gragnaniello V, Carteni-Farina M. Human 5′-deoxy-5′-methylthioadenosine phosphorylase: kinetic studies and catalytic mechanism. Adv Exp Med Biol 1988;250:165–77.
13. Wanders D, Hobson K, Ji X. Methionine restriction and cancer biology. Nutrients 2020;12:684.
14. Li Y, Wang Y, Wu P. 5′-Methylthioadenosine and Cancer: old molecules, new understanding. J Cancer 2019;10:927–36.
15. Marjon K, Cameron MJ, Quang P, Clasquin MF, Mandley E, Kunii K, et al. MTAP deletions in cancer create vulnerability to targeting of the MAT2A/PRMT5/RIOK1 axis. Cell Rep 2016;15:574–87.
16. Mavrakis KJ, McDonald ER III, Schlabach MR, Billy E, Hoffman GR, deWeck A, et al. Disordered methionine metabolism in MTAP/CDKN2A-deleted cancers leads to dependence on PRMT5. Science 2016;351:1208–13.
17. Kryukov GV, Wilson FH, Ruth JR, Paulk J, Tsherniak A, Marlow SE, et al. MTAP deletion confers enhanced dependency on the PRMT5 arginine methyltransferase in cancer cells. Science 2016;351:1214–8.
18. Behrmann I, Wallner S, Komyod W, Heinrich PC, Schuierer M, Buettner R, et al. Characterization of methylthioadenosin phosphorylase (MTAP) expression in malignant melanoma. Am J Pathol 2003;163:683–90.
19. Garcia-Castellano JM, Villanueva A, Healey JH, Sowers R, Cordon-Cardo C, Huvos A, et al. Methylthioadenosine phosphorylase gene deletions are common in osteosarcoma. Clin Cancer Res 2002;8:782–7.
20. Su CY, Chang YC, Chan YC, Lin TC, Huang MS, Yang CJ, et al. MTAP is an independent prognosis marker and the concordant loss of MTAP and p16 expression predicts short survival in non-small cell lung cancer patients. Eur J Surg Oncol 2014;40:1143–50.
21. Abrahao-Machado LF, Antunes B, Filippi RZ, Volc S, Boldrini E, Menezes WP, et al. Loss of MTAP expression is a negative prognostic marker in Ewing sarcoma family of tumors. Biomark Med 2018;12:35–44.
22. Huang HY, Li SH, Yu SC, Chou FF, Tzeng CC, Hu TH, et al. Homozygous deletion of MTAP gene as a poor prognosticator in gastrointestinal stromal tumors. Clin Cancer Res 2009;15:6963–72.
23. Furukawa T, Duguid WP, Rosenberg L, Viallet J, Galloway DA, Tsao MS. Long-term culture and immortalization of epithelial cells from normal adult human pancreatic ducts transfected by the E6E7 gene of human papilloma virus 16. Am J Pathol 1996;148:1763–70.
24. Hong OY, Mou LJ, Luk C, Liu N, Karaskova J, Squire J, et al. Immortal human pancreatic duct epithelial cell lines with near normal genotype and phenotype. Am J Pathol 2000;157:1623–31.
25. Sanjana NE, Shalem O, Zhang F. Improved vectors and genome-wide libraries for CRISPR screening. Nat Methods 2014;11:783–4.
26. Moffat J, Grueneberg DA, Yang X, Kim SY, Kloepfer AM, Hinkle G, et al. A lentiviral RNAi library for human and mouse genes applied to an arrayed viral high-content screen. Cell 2006;124:1283–98.
27. Ji S, Qin Y, Liang C, Huang R, Shi S, Liu J, et al. FBW7 (F-box and WD repeat domain-containing 7) negatively regulates glucose metabolism by targeting the c-Myc/TXNIP (Thioredoxin-Binding Protein) axis in pancreatic cancer. Clin Cancer Res 2016;22:3950–60.
28. Xie G, Wang L, Chen T, Zhou K, Zhang Z, Li J, et al. A metabolite array technology for precision medicine. Anal Chem 2021;93:5709–17.
29. Chong J, Soufan O, Li C, Caraus I, Li S, Bourque G, et al. MetaboAnalyst 4.0: towards more transparent and integrative metabolomics analysis. Nucleic Acids Res 2018;46:W486–w94.
30. Geng H, Harvey CT, Pittsenbarger J, Liu Q, Beer TM, Xue C, et al. HDAC4 protein regulates HIF1alpha protein lysine acetylation and cancer cell response to hypoxia. J Biol Chem 2011;286:38095–102.
31. Huang R, Yu Y, Zong X, Li X, Ma L, Zheng Q. Monomethyltransferase SETD8 regulates breast cancer metabolism via stabilizing hypoxia-inducible factor 1alpha. Cancer Lett 2017;390:1–10.
32. Hu Q, Qin Y, Zhang B, Liang C, Ji S, Shi S, et al. FBW7 increases the chemosensitivity of pancreatic cancer cells to gemcitabine through upregulation of ENT1. Oncol Rep 2017;38:2069–77.
33. Ji S, Qin Y, Shi S, Liu X, Hu H, Zhou H, et al. ERK kinase phosphorylates and destabilizes the tumor suppressor FBW7 in pancreatic cancer. Cell Res 2015;25:561–73.
34. Chou TC, Talalay P. Quantitative analysis of dose-effect relationships: the combined effects of multiple drugs or enzyme inhibitors. Adv Enzyme Regul 1984;22:27–55.
35. Hu Q, Qin Y, Ji S, Xu W, Liu W, Sun Q, et al. UHRF1 promotes aerobic glycolysis and proliferation via suppression of SIRT4 in pancreatic cancer. Cancer Lett 2019;452:226–36.
36. Cerami E, Gao J, Dogrusoz U, Gross BE, Sumer SO, Aksoy BA, et al. The cBio cancer genomics portal: an open platform for exploring multidimensional cancer genomics data. Cancer Discov 2012;2:401–4.
37. Gao J, Aksoy BA, Dogrusoz U, Dresdner G, Gross B, Sumer SO, et al. Integrative analysis of complex cancer genomics and clinical profiles using the cBioPortal. Sci Signal 2013;6:pl1.
38. Sullivan LB, Gui DY, Vander Heiden MG. Altered metabolite levels in cancer: implications for tumour biology and cancer therapy. Nat Rev Cancer 2016;16:680–93.
39. Denko NC. Hypoxia, HIF1 and glucose metabolism in the solid tumour. Nat Rev Cancer 2008;8:705–13.
40. Tang B, Kadariya Y, Chen Y, Slifker M, Kruger WD. Expression of MTAP inhibits tumor-related phenotypes in HT1080 cells via a mechanism unrelated to its enzymatic function. G3 2014;5:35–44.
41. Semenza GL. Regulation of cancer cell metabolism by hypoxia-inducible factor 1. Semin Cancer Biol 2009;19:12–6.
42. Kalev P, Hyer ML, Gross S, Konteatis Z, Chen CC, Fletcher M, et al. MAT2A inhibition blocks the growth of MTAP-deleted cancer cells by reducing PRMT5-dependent mRNA splicing and inducing DNA damage. Cancer Cell 2021;39:209–24.
43. Widmann B, Wandrey F, Badertscher L, Wyler E, Pfannstiel J, Zemp I, et al. The kinase activity of human Rio1 is required for final steps of cytoplasmic maturation of 40S subunits. Mol Biol Cell 2012;23:22–35.
44. Angermayr M, Roidl A, Bandlow W. Yeast Rio1p is the founding member of a novel subfamily of protein serine kinases involved in the control of cell cycle progression. Mol Microbiol 2002;44:309–24.
45. Hamanaka RB, Chandel NS. Targeting glucose metabolism for cancer therapy. J Exp Med 2012;209:211–5.
46. Zhang D, Li J, Wang F, Hu J, Wang S, Sun Y. 2-Deoxy-D-glucose targeting of glucose metabolism in cancer cells as a potential therapy. Cancer Lett 2014;355:176–83.
47. Chou TC. Theoretical basis, experimental design, and computerized simulation of synergism and antagonism in drug combination studies. Pharmacol Rev 2006;58:621–81.
48. Menezes WP, Silva VAO, Gomes INF, Rosa MN, Spina MLC, Carloni AC, et al. Loss of 5′-methylthioadenosine phosphorylase (MTAP) is frequent in high-grade gliomas; nevertheless, it is not associated with higher tumor aggressiveness. Cells 2020;9:492.

49. Yan L, Raj P, Yao W, Ying H. Glucose metabolism in pancreatic cancer. Cancers 2019;11:1460.
50. Kindler HL, Burris HA 3rd, Sandler AB, Oliff IA. A phase II multicenter study of L-alanosine, a potent inhibitor of adenine biosynthesis, in patients with MTAP-deficient cancer. Invest New Drugs 2009;27:75–81.
51. Luengo A, Gui DY, Vander Heiden MG. Targeting metabolism for cancer therapy. Cell Chem Biol 2017;24:1161–80.
52. Sanderson SM, Mikhael PG, Ramesh V, Dai Z, Locasale JW. Nutrient availability shapes methionine metabolism in p16/MTAP-deleted cells. Sci Adv 2019;5: eaav7769.
53. Stopa N, Krebs JE, Shechter D. The PRMT5 arginine methyltransferase: many roles in development, cancer and beyond. Cell Mol Life Sci 2015;72: 2041–59.
54. Mottet D, Michel G, Renard P, Ninane N, Raes M, Michiels C. Role of ERK and calcium in the hypoxia-induced activation of HIF-1. J Cell Physiol 2003; 194:30–44.
55. Nikinmaa M, Pursiheimo S, Soitamo AJ. Redox state regulates HIF-1alpha and its DNA binding and phosphorylation in salmonid cells. J Cell Sci 2004;117: 3201–6.
56. Koyasu S, Kobayashi M, Goto Y, Hiraoka M, Harada H. Regulatory mechanisms of hypoxia-inducible factor 1 activity: two decades of knowledge. Cancer Sci 2018;109:560–71.
57. Warfel NA, Dolloff NG, Dicker DT, Malysz J, El-Deiry WS. CDK1 stabilizes HIF-1alpha via direct phosphorylation of Ser668 to promote tumor growth. Cell Cycle 2013;12:3689–701.
58. Lin A, Li C, Xing Z, Hu Q, Liang K, Han L, et al. The LINK-A lncRNA activates normoxic HIF1alpha signalling in triple-negative breast cancer. Nat Cell Biol 2016;18:213–24.
59. Weinberg F, Reischmann N, Fauth L, Taromi S, Mastroianni J, Kohler M, et al. The atypical kinase RIOK1 promotes tumor growth and invasive behavior. EBioMedicine 2017;20:79–97.
60. Hong X, Huang H, Qiu X, Ding Z, Feng X, Zhu Y, et al. Targeting posttranslational modifications of RIOK1 inhibits the progression of colorectal and gastric cancers. eLife 2018;7:e29511.
61. Yu W, Wang Z, Zhang K, Chi Z, Xu T, Jiang D, et al. One-carbon metabolism supports S-adenosylmethionine and histone methylation to drive inflammatory macrophages. Mol Cell 2019;75:1147–60.
62. Read RD, Fenton TR, Gomez GG, Wykosky J, Vandenberg SR, Babic I, et al. A kinome-wide RNAi screen in Drosophila Glia reveals that the RIO kinases mediate cell proliferation and survival through TORC2-Akt signaling in glioblastoma. PLoS Genet 2013;9:e1003253.
63. Deshpande A, Sicinski P, Hinds PW. Cyclins and cdks in development and cancer: a perspective. Oncogene 2005;24:2909–15.
64. Hirama T, Koeffler HP. Role of the cyclin-dependent kinase inhibitors in the development of cancer. Blood 1995;86:841–54.